

# Average intensity of a partially coherent anomalous hollow beam propagating in underwater oceanic turbulence

DAJUN LIU<sup>\*</sup>, GUIQIU WANG, HAIYANG ZHONG, HONGMING YIN, YAOCHUAN WANG<sup>\*</sup>

Department of Physics, College of Science, Dalian Maritime University, Dalian, 116026, China

\*Corresponding authors: Dajun Liu – liudajun@dlmu.edu.cn; Yaochuan Wang – ycwang@dlmu.edu.cn

Based on the extended Huygens–Fresnel principle, the cross-spectral density function of a partially coherent anomalous hollow beam (AHB) propagating in underwater oceanic turbulence has been derived. The average intensity of partially coherent AHB propagating in underwater oceanic turbulence has been calculated. The influences of coherence length and the strength of underwater oceanic turbulence on the spreading properties of partially coherent AHB are illustrated and analyzed using numerical examples. It is found that the partially coherent AHB with smaller coherence length and the partially coherent AHB propagating in stronger underwater oceanic turbulence will lose the initial beam profile and evolve into the Gaussian beam faster. The results are useful in applications for underwater wireless optical communication.

Keywords: oceanic turbulence, average intensity, anomalous hollow beam.

## 1. Introduction

The dark hollow beam has been widely studied due to its applications in laser optics, atoms optics and optical trapping of particle [1–3]. The propagation properties of a fully coherent dark hollow beam [2] and partially coherent controllable dark hollow beams in turbulent atmosphere [4] have been investigated. The flat-topped vortex hollow beam is another dark hollow beam, and its properties have also been widely studied [5–7]. With the development of laser technology, the anomalous hollow beam of elliptical symmetry with an elliptical solid core was generated in experiment, which provides a powerful tool for studying the linear and nonlinear particle dynamics in the storage ring [8]. Since then, the analytical model to describe the anomalous hollow beam (AHB) has also been introduced [9, 10]. The propagation properties of AHB propagating in free space, the optical system and turbulent media have been widely investigated [11–14] in past years.

The propagation analysis of laser beam in underwater oceanic turbulence is a hot topic, due to its potential applications in underwater wireless optical communication. Recently, the evolution properties of various beams in underwater oceanic turbulence have been widely studied, such as stochastic beams [15], radially polarized beam [16],

stochastic electromagnetic vortex beam [17] and stochastic electromagnetic beam [18], Gaussian Schell-model vortex beam [19], cylindrical vector beam [20], higher order mode laser beam [21], Lorentz and Lorentz–Gauss beams [22–24], four-petal Gaussian beams [25, 26], flat-topped vortex hollow beam [6, 27], pulsed beams [28, 29], linear array beam [30], Gaussian array beam [31–33], and radial phased-locked beam [34, 35]. However, to the best of our knowledge, the properties of partially coherent AHB propagating in underwater oceanic turbulence have not been given. In this paper, the propagation equations of partially coherent AHB in underwater oceanic turbulence have been derived, and the propagation properties of the beam have been investigated using the derived equation.

## 2. Propagation of partially coherent AHB in underwater oceanic turbulence

In the Cartesian coordinate system, the  $z$ -axis is set as the propagation axis, and the cross-spectral density function of a partially coherent anomalous hollow beam (AHB) of elliptical symmetry at the source plane  $z = 0$  can be expressed as follows [36]:

$$\begin{aligned} W(\mathbf{r}_{10}, \mathbf{r}_{20}, 0) &= \left( -2 + \frac{8x_{10}^2}{w_{0x}^2} + \frac{8y_{10}^2}{w_{0y}^2} \right) \exp\left( -\frac{x_{10}^2}{w_{0x}^2} - \frac{y_{10}^2}{w_{0y}^2} \right) \\ &\times \left( -2 + \frac{8x_{20}^2}{w_{0x}^2} + \frac{8y_{20}^2}{w_{0y}^2} \right) \exp\left( -\frac{x_{20}^2}{w_{0x}^2} - \frac{y_{20}^2}{w_{0y}^2} \right) \exp\left[ -\frac{(x_{10} - x_{20})^2}{2\sigma_x^2} - \frac{(y_{10} - y_{20})^2}{2\sigma_y^2} \right] \end{aligned} \quad (1)$$

where  $\mathbf{r}_{10} = (x_{10}, y_{10})$  and  $\mathbf{r}_{20} = (x_{20}, y_{20})$  represent the position vector at the source plane  $z = 0$ ;  $w_{0x}$  and  $w_{0y}$  are the beam waist radius of the astigmatic Gaussian mode in the  $x$ - and  $y$ -axes, respectively;  $\sigma_x$  and  $\sigma_y$  denote the transverse coherence width in  $x$ - and  $y$ -axes, respectively.

The cross-spectral density function of the partially coherent beam propagating in underwater oceanic turbulence can be expressed by the extended Huygens–Fresnel principle [19–34]

$$\begin{aligned} W(\mathbf{r}_1, \mathbf{r}_2, z) &= \frac{k^2}{4\pi^2 z^2} \int_{-\infty}^{+\infty} \int_{-\infty}^{+\infty} \int_{-\infty}^{+\infty} \int_{-\infty}^{+\infty} W(\mathbf{r}_{10}, \mathbf{r}_{20}, 0) \\ &\times \exp\left[ -\frac{ik}{2z} (\mathbf{r}_1 - \mathbf{r}_{10})^2 + \frac{ik}{2z} (\mathbf{r}_2 - \mathbf{r}_{20})^2 \right] \langle \exp[\psi(\mathbf{r}_{10}, \mathbf{r}_1) + \psi^*(\mathbf{r}_{20}, \mathbf{r}_2)] \rangle d\mathbf{r}_{10} d\mathbf{r}_{20} \end{aligned} \quad (2)$$

where  $k = 2\pi/\lambda$  is the wave number with  $\lambda$  being the wavelength;  $\mathbf{r}_1 = (x_1, y_1)$  and  $\mathbf{r}_2 = (x_2, y_2)$  denote the position vector at the receiver plane  $z$ ;  $\psi(\mathbf{r}_0, \mathbf{r})$  is the complex

phase perturbation due to the underwater oceanic turbulence. In Eq. (2), the last term can be written as

$$\langle \exp[\psi(\mathbf{r}_{10}, \mathbf{r}_1) + \psi^*(\mathbf{r}_{20}, \mathbf{r}_2)] \rangle$$

$$= \exp \left\{ -\frac{\pi^2 k^2 z}{3} \int_0^\infty d\kappa \kappa^3 \Phi(\kappa) \left[ (\mathbf{r}_{10} - \mathbf{r}_{20})^2 + (\mathbf{r}_{10} - \mathbf{r}_{20})(\mathbf{r}_1 - \mathbf{r}_2) + (\mathbf{r}_1 - \mathbf{r}_2)^2 \right] \right\} \quad (3)$$

In the above equation, we can define

$$\rho_0^2 = \frac{3}{\pi^2 k^2 z \int_0^\infty d\kappa \kappa^3 \Phi(\kappa)}$$

and  $\kappa$  represents the spatial frequency, and  $\Phi(\kappa)$  is the spatial power spectrum of underwater oceanic turbulence, which can be written as

$$\begin{aligned} \Phi(\kappa) &= 0.388 \times 10^{-8} \varepsilon^{-1/3} \kappa^{-11/3} \left[ 1 + 2.35(\kappa\eta)^{2/3} \right] \\ &\times \frac{\chi_T}{\varsigma^2} \left[ \varsigma^2 \exp(-A_T \delta) + \exp(-A_S \delta) - 2\varsigma \exp(-A_{TS} \delta) \right] \end{aligned} \quad (4)$$

where  $\varepsilon$  denotes the rate of dissipation of kinetic energy per unit mass of fluid, which varies from  $10^{-1}$  to  $10^{-10} \text{ m}^2 \text{s}^{-3}$ ;  $\chi_T$  denotes the rate of dissipation of mean-squared temperature taking the range from  $10^{-4}$  to  $10^{-10} \text{ K}^2 \text{s}^{-1}$ ;  $\varsigma$  represents the ratio of temperature and salinity fluctuations to underwater oceanic turbulence, varying in the range from  $-5$  to  $0$ ,  $0$  value corresponding to the case when salinity-driven turbulence prevails, and  $-5$  value corresponding the case when temperature-driven turbulence dominates. And  $\eta = 10^{-3}$  is the Kolmogorov microscale (inner scale), and  $A_T = 1.863 \times 10^{-2}$ ,  $A_S = 1.9 \times 10^{-4}$ ,  $A_{TS} = 9.41 \times 10^{-3}$ ,  $\delta = 8.284(\kappa\eta)^{4/3} + 12.978(\kappa\eta)^2$ .

Submitting Eq. (1) into Eq. (2), we can derive

$$\begin{aligned} W(\mathbf{r}_1, \mathbf{r}_2, z) &= \frac{k^2}{4\pi^2 z^2} \exp \left[ -\frac{ik}{2z} (x_1^2 + y_1^2 - x_2^2 - y_2^2) \right] \exp \left[ -\frac{(x_1 - x_2)^2 + (y_1 - y_2)^2}{\rho_0^2} \right] \\ &\times \left( 4I_1 - \frac{16}{w_{0x}^2} I_2 - \frac{16}{w_{0y}^2} I_3 - \frac{16}{w_{0x}^2} I_4 - \frac{16}{w_{0y}^2} I_5 + \frac{64}{w_{0x}^4} I_6 + \frac{64}{w_{0x}^2 w_{0y}^2} I_7 \right. \\ &\quad \left. + \frac{64}{w_{0x}^2 w_{0y}^2} I_8 + \frac{64}{w_{0y}^4} I_9 \right) \end{aligned} \quad (5)$$

where:

$$\begin{aligned} I_1 &= \sqrt{\frac{\pi}{a_x}} \exp \left[ \frac{1}{a_x} \left( \frac{ik}{2z} x_1 - \frac{x_1 - x_2}{2\rho_0^2} \right)^2 \right] \sqrt{\frac{\pi}{b_x}} \exp \left( \frac{c_x^2}{b_x} \right) \\ &\quad \times \sqrt{\frac{\pi}{a_y}} \exp \left[ \frac{1}{a_y} \left( \frac{ik}{2z} y_1 - \frac{y_1 - y_2}{2\rho_0^2} \right)^2 \right] \sqrt{\frac{\pi}{b_y}} \exp \left( \frac{c_y^2}{b_y} \right) \end{aligned} \quad (6)$$

$$\begin{aligned} I_2 &= \sqrt{\frac{\pi}{a_x}} 2! \left( \frac{1}{a_x} \right)^2 \exp \left[ \frac{1}{a_x} \left( \frac{ik}{2z} x_1 - \frac{x_1 - x_2}{2\rho_0^2} \right)^2 \right] \sum_{l=0}^1 \frac{1}{l!(2-2l)!} \left( \frac{a_x}{4} \right)^l \\ &\quad \times \sum_{s=0}^{2-2l} \frac{(2-2l)!}{s!(2-2l-s)!} \left( \frac{ik}{2z} x_1 - \frac{x_1 - x_2}{2\rho_0^2} \right)^{2-2l-s} \left( \frac{1}{2\sigma_x^2} + \frac{1}{\rho_0^2} \right)^s \\ &\quad \times \sqrt{\frac{\pi}{b_x}} 2^{-s} i^s \exp \left( \frac{c_x^2}{b_x} \right) \left( \frac{1}{b_x} \right)^{0.5s} H_s \left( -\frac{ic_x}{\sqrt{b_x}} \right) \\ &\quad \times \sqrt{\frac{\pi}{a_y}} \exp \left[ \frac{1}{a_y} \left( \frac{ik}{2z} y_1 - \frac{y_1 - y_2}{2\rho_0^2} \right)^2 \right] \sqrt{\frac{\pi}{b_y}} \exp \left( \frac{c_y^2}{b_y} \right) \end{aligned} \quad (7)$$

$$\begin{aligned} I_3 &= \sqrt{\frac{\pi}{a_x}} \exp \left[ \frac{1}{a_x} \left( \frac{ik}{2z} x_1 - \frac{x_1 - x_2}{2\rho_0^2} \right)^2 \right] \sqrt{\frac{\pi}{b_x}} \exp \left( \frac{c_x^2}{b_x} \right) \\ &\quad \times \sqrt{\frac{\pi}{a_y}} 2! \left( \frac{1}{a_y} \right)^2 \exp \left[ \frac{1}{a_y} \left( \frac{ik}{2z} y_1 - \frac{y_1 - y_2}{2\rho_0^2} \right)^2 \right] \sum_{l=0}^1 \frac{1}{l!(2-2l)!} \left( \frac{a_y}{4} \right)^l \\ &\quad \times \sum_{s=0}^{2-2l} \frac{(2-2l)!}{s!(2-2l-s)!} \left( \frac{ik}{2z} y_1 - \frac{y_1 - y_2}{2\rho_0^2} \right)^{2-2l-s} \left( \frac{1}{2\sigma_y^2} + \frac{1}{\rho_0^2} \right)^s \\ &\quad \times \sqrt{\frac{\pi}{b_y}} 2^{-s} i^s \exp \left( \frac{c_y^2}{b_y} \right) \left( \frac{1}{b_y} \right)^{0.5s} H_s \left( -\frac{ic_y}{\sqrt{b_y}} \right) \end{aligned} \quad (8)$$

$$\begin{aligned} I_4 &= \sqrt{\frac{\pi}{a_x}} \exp \left[ \frac{1}{a_x} \left( \frac{ik}{2z} x_1 - \frac{x_1 - x_2}{2\rho_0^2} \right)^2 \right] \sqrt{\frac{\pi}{b_x}} 2^{-2} i^2 \exp \left( \frac{c_x^2}{b_x} \right) \left( \frac{1}{b_x} \right) H_2 \left( -\frac{ic_x}{\sqrt{b_x}} \right) \\ &\quad \times \sqrt{\frac{\pi}{a_y}} \exp \left[ \frac{1}{a_y} \left( \frac{ik}{2z} y_1 - \frac{y_1 - y_2}{2\rho_0^2} \right)^2 \right] \sqrt{\frac{\pi}{b_y}} \exp \left( \frac{c_y^2}{b_y} \right) \end{aligned} \quad (9)$$

$$\begin{aligned}
I_5 = & \sqrt{\frac{\pi}{a_x}} \exp \left[ \frac{1}{a_x} \left( \frac{ik}{2z} x_1 - \frac{x_1 - x_2}{2\rho_0^2} \right)^2 \right] \sqrt{\frac{\pi}{b_x}} \exp \left( \frac{c_x^2}{b_x} \right) \\
& \times \sqrt{\frac{\pi}{a_y}} \exp \left[ \frac{1}{a_y} \left( \frac{ik}{2z} y_1 - \frac{y_1 - y_2}{2\rho_0^2} \right)^2 \right] \\
& \times \sqrt{\frac{\pi}{b_y}} 2^{-2} i^2 \exp \left( \frac{c_y^2}{b_y} \right) \left( \frac{1}{b_y} \right) H_2 \left( -\frac{ic_y}{\sqrt{b_y}} \right)
\end{aligned} \tag{10}$$

$$\begin{aligned}
I_6 = & \sqrt{\frac{\pi}{a_x}} 2! \left( \frac{1}{a_x} \right)^2 \exp \left[ \frac{1}{a_x} \left( \frac{ik}{2z} x_1 - \frac{x_1 - x_2}{2\rho_0^2} \right)^2 \right] \sum_{l=0}^1 \frac{1}{l!(2-2l)!} \left( \frac{a_x}{4} \right)^l \\
& \times \sum_{s=0}^{2-2l} \frac{(2-2l)!}{s!(2-2l-s)!} \left( \frac{ik}{2z} x_1 - \frac{x_1 - x_2}{2\rho_0^2} \right)^{2-2l-s} \left( \frac{1}{2\sigma_x^2} + \frac{1}{\rho_0^2} \right)^s \\
& \times \sqrt{\frac{\pi}{b_x}} 2^{-2-s} i^{2+s} \exp \left( \frac{c_x^2}{b_x} \right) \left( \frac{1}{b_x} \right)^{0.5(2+s)} H_{2+s} \left( -\frac{ic_x}{\sqrt{b_x}} \right) \\
& \times \sqrt{\frac{\pi}{a_y}} \exp \left[ \frac{1}{a_y} \left( \frac{ik}{2z} y_1 - \frac{y_1 - y_2}{2\rho_0^2} \right)^2 \right] \sqrt{\frac{\pi}{b_y}} \exp \left( \frac{c_y^2}{b_y} \right)
\end{aligned} \tag{11}$$

$$\begin{aligned}
I_7 = & \sqrt{\frac{\pi}{a_x}} 2! \left( \frac{1}{a_x} \right)^2 \exp \left[ \frac{1}{a_x} \left( \frac{ik}{2z} x_1 - \frac{x_1 - x_2}{2\rho_0^2} \right)^2 \right] \sum_{l=0}^1 \frac{1}{l!(2-2l)!} \left( \frac{a_x}{4} \right)^l \\
& \times \sum_{s=0}^{2-2l} \frac{(2-2l)!}{s!(2-2l-s)!} \left( \frac{ik}{2z} x_1 - \frac{x_1 - x_2}{2\rho_0^2} \right)^{2-2l-s} \left( \frac{1}{2\sigma_x^2} + \frac{1}{\rho_0^2} \right)^s \\
& \times \sqrt{\frac{\pi}{b_x}} 2^{-s} i^s \exp \left( \frac{c_x^2}{b_x} \right) \left( \frac{1}{b_x} \right)^{0.5s} H_s \left( -\frac{ic_x}{\sqrt{b_x}} \right) \\
& \times \sqrt{\frac{\pi}{a_y}} \exp \left[ \frac{1}{a_y} \left( \frac{ik}{2z} y_1 - \frac{y_1 - y_2}{2\rho_0^2} \right)^2 \right] \\
& \times \sqrt{\frac{\pi}{b_y}} 2^{-2} i^2 \exp \left( \frac{c_y^2}{b_y} \right) \left( \frac{1}{b_y} \right) H_2 \left( -\frac{ic_y}{\sqrt{b_y}} \right)
\end{aligned} \tag{12}$$

$$\begin{aligned}
I_8 = & \sqrt{\frac{\pi}{a_x}} \exp \left[ \frac{1}{a_x} \left( \frac{ik}{2z} x_1 - \frac{x_1 - x_2}{2\rho_0^2} \right)^2 \right] \sqrt{\frac{\pi}{b_x}} 2^{-2} i^2 \exp \left( \frac{c_x^2}{b_x} \right) \left( \frac{1}{b_x} \right) H_2 \left( -\frac{ic_x}{\sqrt{b_x}} \right) \\
& \times \sqrt{\frac{\pi}{a_y}} 2! \left( \frac{1}{a_y} \right)^2 \exp \left[ \frac{1}{a_y} \left( \frac{ik}{2z} y_1 - \frac{y_1 - y_2}{2\rho_0^2} \right)^2 \right] \sum_{l=0}^1 \frac{1}{l!(2-2l)!} \left( \frac{a_y}{4} \right)^l \\
& \times \sum_{s=0}^{2-2l} \frac{(2-2l)!}{s!(2-2l-s)!} \left( \frac{ik}{2z} y_1 - \frac{y_1 - y_2}{2\rho_0^2} \right)^{2-2l-s} \left( \frac{1}{2\sigma_y^2} + \frac{1}{\rho_0^2} \right)^s \\
& \times \sqrt{\frac{\pi}{b_y}} 2^{-s} i^s \exp \left( \frac{c_y^2}{b_y} \right) \left( \frac{1}{b_y} \right)^{0.5s} H_s \left( -\frac{ic_y}{\sqrt{b_y}} \right)
\end{aligned} \tag{13}$$

$$\begin{aligned}
I_9 = & \sqrt{\frac{\pi}{a_x}} \exp \left[ \frac{1}{a_x} \left( \frac{ik}{2z} x_1 - \frac{x_1 - x_2}{2\rho_0^2} \right)^2 \right] \sqrt{\frac{\pi}{b_x}} \exp \left( \frac{c_x^2}{b_x} \right) \\
& \times \sqrt{\frac{\pi}{a_y}} 2! \left( \frac{1}{a_y} \right)^2 \exp \left[ \frac{1}{a_y} \left( \frac{ik}{2z} y_1 - \frac{y_1 - y_2}{2\rho_0^2} \right)^2 \right] \sum_{l=0}^1 \frac{1}{l!(2-2l)!} \left( \frac{a_y}{4} \right)^l \\
& \times \sum_{s=0}^{2-2l} \frac{(2-2l)!}{s!(2-2l-s)!} \left( \frac{ik}{2z} y_1 - \frac{y_1 - y_2}{2\rho_0^2} \right)^{2-2l-s} \left( \frac{1}{2\sigma_y^2} + \frac{1}{\rho_0^2} \right)^s \\
& \times \sqrt{\frac{\pi}{b_y}} 2^{-2-s} i^{2+s} \exp \left( \frac{c_y^2}{b_y} \right) \left( \frac{1}{b_y} \right)^{0.5(2+s)} H_{2+s} \left( -\frac{ic_y}{\sqrt{b_y}} \right)
\end{aligned} \tag{14}$$

with

$$a_\beta = \frac{1}{w_{0\beta}^2} + \frac{1}{2\sigma_\beta^2} + \frac{ik}{2z} + \frac{1}{\rho_0^2}, \quad (\beta = x, y) \tag{15}$$

$$b_\beta = \frac{1}{w_{0\beta}^2} + \frac{1}{2\sigma_\beta^2} - \frac{ik}{2z} + \frac{1}{\rho_0^2} - \frac{1}{a_\beta} \left( \frac{1}{2\sigma_\beta^2} + \frac{1}{\rho_0^2} \right)^2 \tag{16}$$

$$c_\beta = \frac{1}{a_\beta} \left( \frac{ik}{2z} \beta_1 - \frac{\beta_1 - \beta_2}{2\rho_0^2} \right) \left( \frac{1}{2\sigma_\beta^2} + \frac{1}{\rho_0^2} \right) + \frac{\beta_1 - \beta_2}{2\rho_0^2} - \frac{ik}{2z} \beta_2 \tag{17}$$

In the derivations of the above equations, the following integral formula have been used [37]:

$$\begin{aligned} & \int_{-\infty}^{+\infty} x^n \exp(-px^2 + 2qx) dx \\ &= n! \exp\left(\frac{q^2}{p}\right) \left(\frac{q}{p}\right)^n \sqrt{\frac{\pi}{p}} \sum_{k=0}^{\left[\frac{n}{2}\right]} \frac{1}{k!(n-2k)!} \left(\frac{p}{4q^2}\right)^k \end{aligned} \quad (18)$$

$$H_{2d}(x) = \sum_{l=0}^d \frac{(-1)^l (2d)!}{l!(2d-2l)!} (2x)^{2d-2l} \quad (19)$$

Equations (5)–(17) are the main obtained equations of this paper. The propagation properties of the partially coherent AHB in underwater oceanic turbulence can be simulated using the derived equations.

### 3. Numerical simulations and discussions

The average intensity properties of partially coherent AHB propagating in underwater oceanic turbulence are illustrated and analyzed in this section. In the following numerical calculations, unless specified otherwise, the parameters of partially coherent AHB and underwater oceanic turbulence are chosen as  $\lambda = 417 \text{ nm}$ ,  $w_{0x} = w_{0y} = w_0 = 1 \text{ cm}$ ,  $\sigma_x = \sigma_y = \sigma = 1 \text{ cm}$ ,  $\chi_T = 10^{-8} \text{ K}^2 \text{s}^{-1}$ ,  $\varepsilon = 10^{-7} \text{ m}^2 \text{s}^{-3}$ , and  $\zeta = -2.5$ .

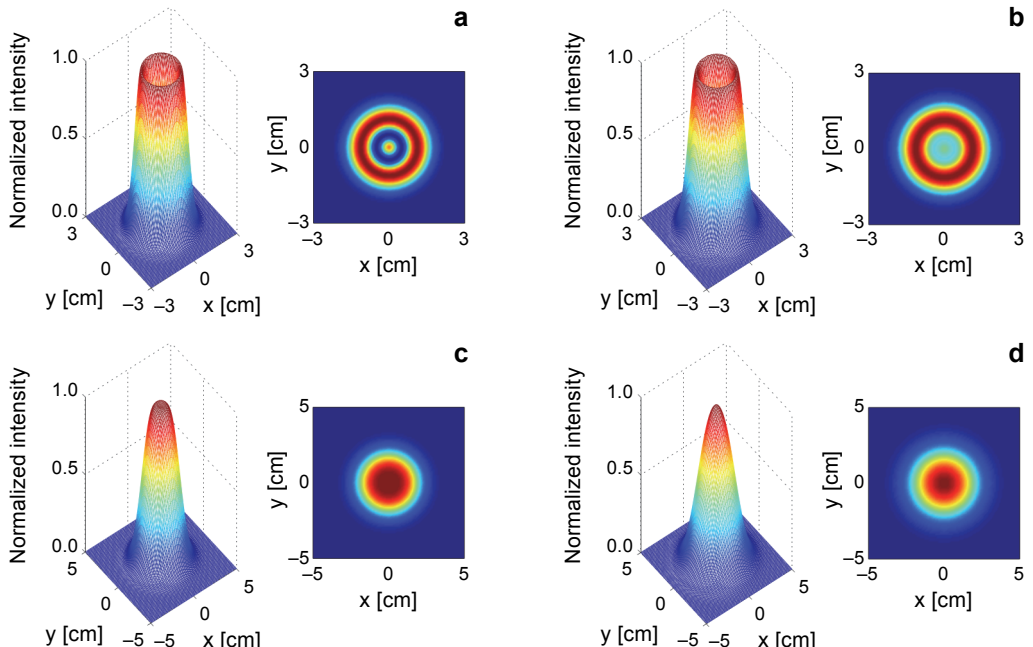


Fig. 1. Normalized intensity of a partially coherent circular AHB propagating in underwater oceanic turbulence;  $z = 20 \text{ m}$  (a),  $z = 80 \text{ m}$  (b),  $z = 160 \text{ m}$  (c), and  $z = 200 \text{ m}$  (d).

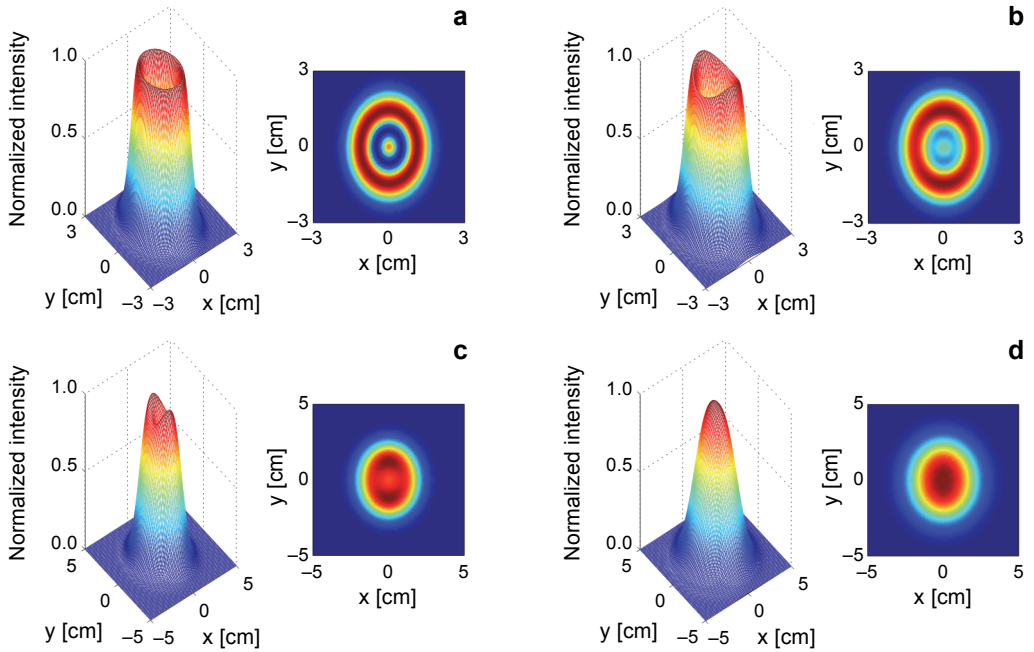


Fig. 2. Normalized intensity of a partially coherent elliptical AHB propagating in underwater oceanic turbulence;  $z = 20$  m (a),  $z = 80$  m (b),  $z = 150$  m (c), and  $z = 200$  m (d).

The normalized average intensity and contour graphs of a partially coherent circular and elliptical AHB propagating in underwater oceanic turbulence are illustrated in Figs. 1 and 2, respectively. And the parameters in Fig. 2 are chosen as  $w_{0x} = 1$  cm and  $w_{0y} = 1.3$  cm. At the short propagation distance, the beam profiles (hollow beam with a solid core) of a partially coherent circular and elliptical AHB are kept the same as the beam at the source plane [35]. As the propagation distance increases, the partially coherent AHB propagating in underwater oceanic turbulence will lose its solid core, and evolve into the Gaussian beam (Figs. 1d and 2d) at a longer propagation distance. One can also see from Fig. 1 that the partially coherent circular AHB can become the flat-topped beam (Fig. 1c), before the beam evolves into the Gaussian beam. From the previous reports [38], we know that the flat-topped beam propagating in random media will evolve into the Gaussian beam as the propagation distance increases.

The influences of coherence length  $\sigma_x = \sigma_y = \sigma$  on the propagation properties of a partially coherent circular AHB propagating in underwater oceanic turbulence are shown in Fig. 3. One sees from Fig. 3 that the fully coherent AHB propagating in underwater oceanic turbulence will lose its initial beam profile slower than the partially coherent AHB with smaller coherence length. So, the fully coherent AHB should be chosen as the beam profiles of AHB are needed in underwater environment.

In order to investigate the influences of underwater oceanic turbulence on the average intensity of a partially coherent AHB, Figs. 4–6 show the cross-sections of normalized intensity of a partially coherent circular AHB with  $\sigma_x = \sigma_y = 1$  mm propagating in un-

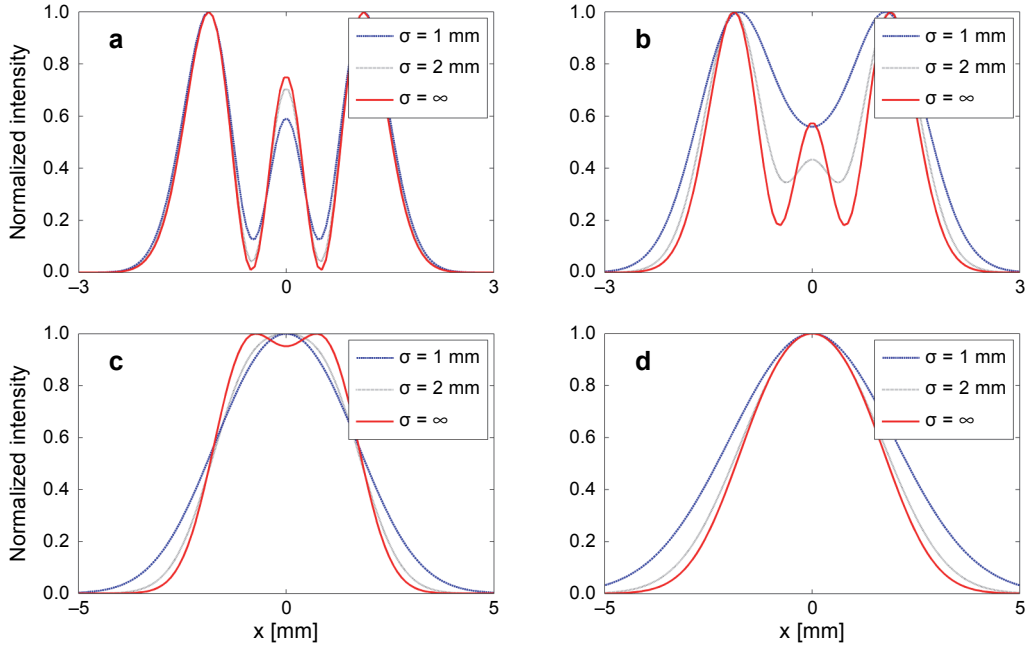


Fig. 3. Cross-sections of normalized intensity of a partially coherent circular AHB propagating in underwater oceanic turbulence for different  $\sigma$ ;  $z = 20 \text{ m}$  (a),  $z = 60 \text{ m}$  (b),  $z = 150 \text{ m}$  (c), and  $z = 200 \text{ m}$  (d).

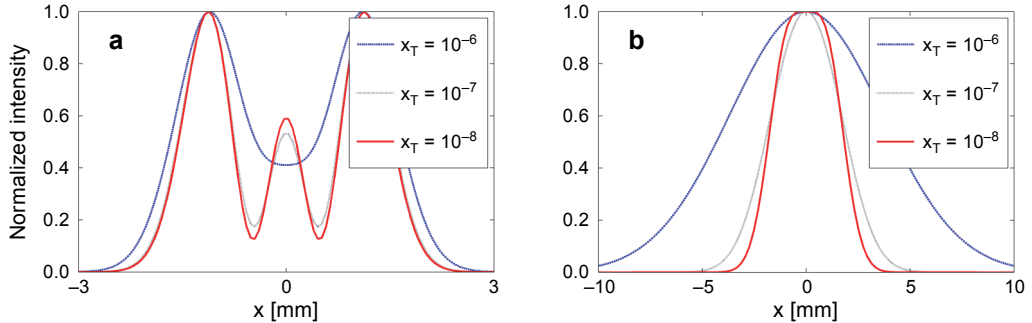


Fig. 4. Cross-sections of normalized intensity of a partially coherent circular AHB propagating in underwater oceanic turbulence for different  $x_T$ ;  $z = 20 \text{ m}$  (a), and  $z = 100 \text{ m}$  (b).

derwater oceanic turbulence for different  $\chi_T$ ,  $\varepsilon$ , and  $\zeta$ , respectively. One sees from Fig. 4 that the partially coherent AHB propagating in underwater oceanic turbulence with larger  $\chi_T$  will lose its initial beam profile at the short propagation distance (Fig. 4a); with increasing propagation distance, partially coherent AHB will gradually lose its initial beam profile and evolve into the Gaussian beam as the underwater oceanic turbulence  $\chi_T$  increases. The phenomena can be explained that the strength of underwater oceanic turbulence will become stronger as the underwater oceanic turbulence  $\chi_T$  increases. From Figs. 5 and 6, it is also found that the partially coherent AHB propagating

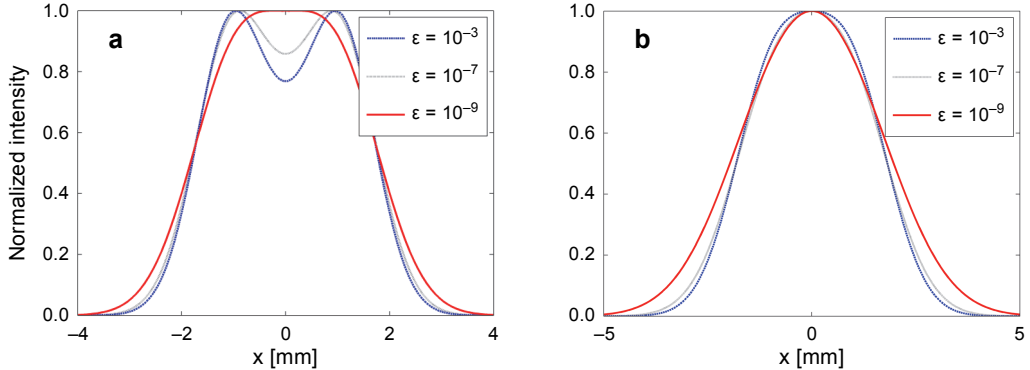


Fig. 5. Cross-sections of normalized intensity of a partially coherent circular AHB propagating in underwater oceanic turbulence for different  $\varepsilon$ ;  $z = 80 \text{ m}$  (a), and  $z = 120 \text{ m}$  (b).

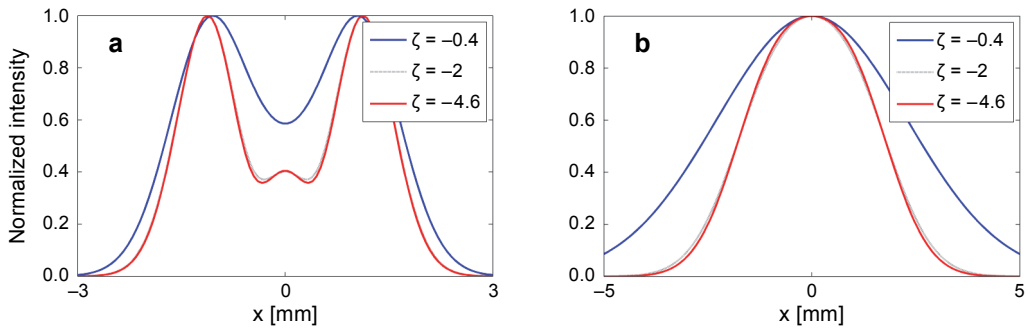


Fig. 6. Cross-sections of normalized intensity of a partially coherent circular AHB propagating in underwater oceanic turbulence for different  $\zeta$ ;  $z = 40 \text{ m}$  (a), and  $z = 120 \text{ m}$  (b).

in underwater oceanic turbulence with smaller  $\varepsilon$  (Fig. 5a) or larger  $\zeta$  (Fig. 6a) will lose its initial beam profile at the short propagation distance, and the beam will evolve into the Gaussian beam faster with the  $\varepsilon$  decreasing or  $\zeta$  increasing at the beam propagation in underwater oceanic turbulence. The spreading properties of partially coherent AHB propagating in underwater oceanic turbulence can be characterized by the fact that the beam propagating in stronger underwater oceanic turbulence (the increase of underwater oceanic turbulence parameters  $\chi_T$  and  $\zeta$  or the decrease of underwater oceanic turbulence parameter  $\varepsilon$ ) will lose its initial beam profile and evolve into the Gaussian beam faster.

#### 4. Conclusions

The cross-spectral density function of a partially coherent AHB propagating in underwater oceanic turbulence has been derived, and the evolution properties of average in-

tensity for a partially coherent AHB propagating in underwater oceanic turbulence have been illustrated and analyzed based on the derived equations. The results show that the partially coherent AHB propagating in underwater oceanic turbulence will lose its solid core, and evolve into the Gaussian beam as the propagation distance increases; and the partially coherent AHB with smaller coherence length will evolve into the Gaussian beam more rapidly. And it is also found that the partially coherent AHB propagating in stronger underwater oceanic turbulence (the increase of underwater oceanic turbulence parameters  $\chi_T$  and  $\varsigma$  or the decrease of underwater oceanic turbulence parameter  $\varepsilon$ ) will lose its initial beam profile and evolve into the Gaussian beam faster.

*Acknowledgements* – This work was supported by National Natural Science Foundation of China (11604038, 11404048, 11375034), Natural Science Foundation of Liaoning Province (201602062, 201602061) and the Fundamental Research Funds for the Central Universities (3132019182, 3132019184, 3132018235, 3132018236).

## References

- [1] CAI Y., CHEN C., WANG F., *Modified hollow Gaussian beam and its paraxial propagation*, Optics Communications **278**(1), 2007, pp. 34–41, DOI: 10.1016/j.optcom.2007.06.012.
- [2] CHEN Y., CAI Y., EYYUBOĞLU H.T., BAYKAL Y., *Scintillation properties of dark hollow beams in a weak turbulent atmosphere*, Applied Physics B **90**(1), 2008, pp. 87–92, DOI: 10.1007/s00340-007-2825-1.
- [3] LIU D., ZHOU Z., *Various dark hollow beams propagating in uniaxial crystals orthogonal to the optical axis*, Journal of Optics A: Pure and Applied Optics **10**(9), 2008, article ID 095005, DOI: 10.1088/1464-4258/10/9/095005.
- [4] WANG H., LI X., *Propagation of partially coherent controllable dark hollow beams with various symmetries in turbulent atmosphere*, Optics and Lasers in Engineering **48**(1), 2010, pp. 48–57, DOI: 10.1016/j.optlaseng.2009.07.014.
- [5] LIU D., WANG Y., WANG G., YIN H., *Propagation properties of a partially coherent flat-topped vortex hollow beam in turbulent atmosphere*, Journal of the Optical Society of Korea **20**(1), 2016, pp. 1–7.
- [6] LIU D., WANG Y., YIN H., *Evolution properties of partially coherent flat-topped vortex hollow beam in oceanic turbulence*, Applied Optics **54**(35), 2015, pp. 10510–10516, DOI: 10.1364/AO.54.010510.
- [7] LIU D., WANG G., LUO X., YIN H., WANG Y., *Evolution properties of a partially coherent flat-topped vortex hollow beam propagating in uniaxial crystals orthogonal to the optical axis*, Journal of the Optical Society of Korea **20**(6), 2016, pp. 686–693.
- [8] WU Y., LI J., WU J., *Anomalous hollow electron beams in a storage ring*, Physical Review Letters **94**(13), 2005, article ID 134802, DOI: 10.1103/PhysRevLett.94.134802.
- [9] CAI Y., *Model for an anomalous hollow beam and its paraxial propagation*, Optics Letters **32**(21), 2007, pp. 3179–3181, DOI: 10.1364/OL.32.003179.
- [10] CAI Y., WANG Z., LIN Q., *An alternative theoretical model for an anomalous hollow beam*, Optics Express **16**(19), 2008, pp. 15254–15267, DOI: 10.1364/OE.16.015254.
- [11] LIU D., ZHOU Z., *Analytical vectorial structure of the anomalous hollow beam in the far field*, Optics and Laser Technology **42**(4), 2010, pp. 640–646, DOI: 10.1016/j.optlastec.2009.11.003.
- [12] WANG K., ZHAO C., XU B., *Propagation of anomalous hollow beam through a misaligned first-order optical system*, Optics and Laser Technology **42**(8), 2010, pp. 1218–1222, DOI: 10.1016/j.optlastec.2010.03.013.
- [13] LU X., ZHU X., WANG K., ZHAO C., CAI Y., *Effects of biological tissues on the propagation properties of anomalous hollow beams*, Optik **127**(4), 2016, pp. 1842–1847, DOI: 10.1016/j.jleo.2015.11.039.

- [14] TIAN H., XU Y., YANG T., MA Z., WANG S., DAN Y., *Propagation characteristics of partially coherent anomalous elliptical hollow Gaussian beam propagating through atmospheric turbulence along a slant path*, Journal of Modern Optics **64**(4), 2017, pp. 422–429, DOI: 10.1080/09500340.2016.1241441.
- [15] KOROTKOVA O., FARWELL N., *Effect of oceanic turbulence on polarization of stochastic beams*, Optics Communications **284**(7), 2011, pp. 1740–1746, DOI: 10.1016/j.optcom.2010.12.024.
- [16] TANG M., ZHAO D., *Propagation of radially polarized beams in the oceanic turbulence*, Applied Physics B **111**(4), 2013, pp. 665–670, DOI: 10.1007/s00340-013-5394-5.
- [17] XU J., ZHAO D., *Propagation of a stochastic electromagnetic vortex beam in the oceanic turbulence*, Optics and Laser Technology **57**, 2014, pp. 189–193, DOI: 10.1016/j.optlastec.2013.10.019.
- [18] ZHOU Y., CHEN Q., ZHAO D., *Propagation of astigmatic stochastic electromagnetic beams in oceanic turbulence*, Applied Physics B **114**(4), 2014, pp. 475–482, DOI: 10.1007/s00340-013-5545-8.
- [19] HUANG Y., ZHANG B., GAO Z., ZHAO G., DUAN Z., *Evolution behavior of Gaussian Schell-model vortex beams propagating through oceanic turbulence*, Optics Express **22**(15), 2014, pp. 17723–17734, DOI: 10.1364/OE.22.017723.
- [20] DONG Y., GUO L., LIANG C., WANG F., CAI Y., *Statistical properties of a partially coherent cylindrical vector beam in oceanic turbulence*, Journal of the Optical Society of America A **32**(5), 2015, pp. 894–901, DOI: 10.1364/JOSAA.32.000894.
- [21] BAYKAL Y., *Higher order mode laser beam intensity fluctuations in strong oceanic turbulence*, Optics Communications **390**, 2017, pp. 72–75, DOI: 10.1016/j.optcom.2016.12.072.
- [22] LIU D., WANG Y., *Average intensity of a Lorentz beam in oceanic turbulence*, Optik **144**, 2017, pp. 76–85, DOI: 10.1016/j.ijleo.2017.06.078.
- [23] LIU D., WANG G., WANG Y., *Average intensity and coherence properties of a partially coherent Lorentz–Gauss beam propagating through oceanic turbulence*, Optics and Laser Technology **98**, 2018, pp. 309–317, DOI: 10.1016/j.optlastec.2017.08.011.
- [24] LIU D., YIN H., WANG G., WANG Y., *Propagation of partially coherent Lorentz–Gauss vortex beam through oceanic turbulence*, Applied Optics **56**(31), 2017, pp. 8785–8792, DOI: 10.1364/AO.56.0.08785.
- [25] LIU D., WANG Y., LUO X., WANG G., YIN H., *Evolution properties of partially coherent four-petal Gaussian beams in oceanic turbulence*, Journal of Modern Optics **64**(16), 2017, pp. 1579–1587, DOI: 10.1080/09500340.2017.1300698.
- [26] LIU D., WANG Y., WANG G., LUO X., YIN H., *Propagation properties of partially coherent four-petal Gaussian vortex beams in oceanic turbulence*, Laser Physics **27**(1), 2017, article ID 016001, DOI: 10.1088/1555-6611/27/1/016001.
- [27] LIU D., CHEN L., WANG Y., WANG G., YIN H., *Average intensity properties of flat-topped vortex hollow beam propagating through oceanic turbulence*, Optik **127**(17), 2016, pp. 6961–6969, DOI: 10.1016/j.ijleo.2016.04.142.
- [28] LIU D., WANG Y., WANG G., YIN H., WANG J., *The influence of oceanic turbulence on the spectral properties of chirped Gaussian pulsed beam*, Optics and Laser Technology **82**, 2016, pp. 76–81, DOI: 10.1016/j.optlastec.2016.02.019.
- [29] WANG Z., LU L., ZHANG P., FAN C., JI X., *Broadening of ultra-short pulses propagating through weak-to-strong oceanic turbulence*, Optics Communications **367**, 2016, pp. 95–101, DOI: 10.1016/j.optcom.2016.01.013.
- [30] HUANG Y., HUANG P., WANG F., ZHAO G., ZENG A., *The influence of oceanic turbulence on the beam quality parameters of partially coherent Hermite–Gaussian linear array beams*, Optics Communications **336**, 2015, pp. 146–152, DOI: 10.1016/j.optcom.2014.09.055.
- [31] LU L., WANG Z., ZHANG J., ZHANG P., QIAO C., FAN C., JI X., *Average intensity of  $M \times N$  Gaussian array beams in oceanic turbulence*, Applied Optics **54**(25), 2015, pp. 7500–7507, DOI: 10.1364/AO.54.007500.
- [32] TANG M., ZHAO D., *Regions of spreading of Gaussian array beams propagating through oceanic turbulence*, Applied Optics **54**(11), 2015, pp. 3407–3411, DOI: 10.1364/AO.54.003407.

- [33] LU L., ZHANG P., FAN C., QIAO C., *Influence of oceanic turbulence on propagation of a radial Gaussian beam array*, Optics Express **23**(3), 2015, pp. 2827–2836, DOI: 10.1364/OE.23.002827.
- [34] LIU D., WANG Y., *Evolution properties of a radial phased-locked partially coherent Lorentz–Gauss array beam in oceanic turbulence*, Optics and Laser Technology **103**, 2018, pp. 33–41, DOI: 10.1016/j.optlastec.2018.01.014.
- [35] YOUSEFI M., KASHANI F.D., MASHAL A., *Analyzing the average intensity distribution and beam width evolution of phase-locked partially coherent radial flat-topped array laser beams in oceanic turbulence*, Laser Physics **27**(2), 2017, article ID 026202, DOI: 10.1088/1555-6611/aa4f58.
- [36] CAI Y., WANG F., *Partially coherent anomalous hollow beam and its paraxial propagation*, Physics Letters A **372**(25), 2008, pp. 4654–4660, DOI: 10.1016/j.physleta.2008.05.005.
- [37] JEFFREY H.D.A., *Handbook of Mathematical Formulas and Integrals*, Fourth Ed., Academic Press, 2008.
- [38] CAI Y., *Propagation of various flat-topped beams in a turbulent atmosphere*, Journal of Optics A: Pure and Applied Optics **8**(6), 2006, pp. 537–545, DOI: 10.1088/1464-4258/8/6/008.

Received April 20, 2018  
in revised form June 5, 2018